

# System-Aware Compression

Yehuda Dar, Michael Elad, and Alfred M. Bruckstein  
Computer Science Department, Technion – Israel Institute of Technology  
{ydar,elad,freddy}@cs.technion.ac.il

**Abstract**—Many information systems employ lossy compression as a crucial intermediate stage among other processing components. While the important distortion is defined by the system’s input and output signals, the compression usually ignores the system structure, therefore, leading to an overall sub-optimal rate-distortion performance. In this paper we propose a compression methodology for an operational rate-distortion optimization considering a known system layout, modeled using linear operators and noise. Using the alternating direction method of multipliers (ADMM) technique, we show that the design of the new globally-optimized compression reduces to a standard compression of a “system adjusted” signal. Essentially, the proposed framework leverages standard compression techniques to address practical settings of the noisy source coding problem. We further explain the main ideas of our method by theoretically studying the case of a cyclo-stationary Gaussian signal. We present experimental results for coding of one-dimensional signals and for video compression using the HEVC standard, showing significant gains by the adjustment to an acquisition-rendering system.

## I. INTRODUCTION

Lossy compression has a central role in information systems where the data may be inaccurately represented in order to meet storage-space or transmission-bandwidth constraints. While the compression is a crucial system-component, it is only an intermediate stage among data processing procedures that determine the eventual output of the system. For example, consider a common audio/visual system structure where the source signal is acquired and compressed for its storage/transmission, then the decompression is followed by a rendering stage producing the ultimate system output. Evidently, in this example, the quality of the system output is determined by the acquisition-rendering chain, and not solely on the lossy compression stage. Nevertheless, the compression is usually designed independently of the system structure, thus inducing a sub-optimal rate-distortion performance for the complete system.

Here we propose a compression approach defined by an operational rate-distortion optimization considering a known system structure. Specifically, we study a general flow (Fig. 1) where the compression is preceded by a linear operator distorting the input along with an additive white noise, and the decompression is followed by another linear operation. We formulate a rate-distortion optimization based on a quadratic distortion metric involving the system’s linear operators. For general linear operators, this intricate rate-distortion optimization is too hard to be directly solved for high dimensional signals. Consequently, we address this challenge using the alternating direction method of multipliers (ADMM) technique [1], suggesting an iterative procedure that relies on the simpler

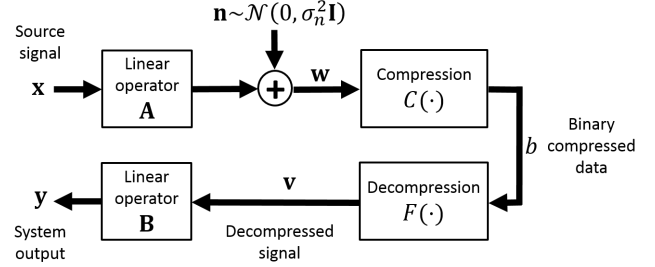


Fig. 1. The general system structure considered in this paper.

tasks of standard compression (which is system independent!) and  $\ell_2$ -constrained deconvolution for the linear operators of the system.

Optimizing the system output quality from the compression standpoint is an attractive answer to the inherent tradeoff among distortion, bit-cost, and computational complexity. First, bits are wisely spent for representing signal components that will be important at the output of the overall system (for example, one should obviously not code signal components belonging to the null space of the post-decompression operator). Second, the added computational load can be well accommodated in the compression environment that is often rich in computational and time resources, in contrast to the decompression stage.

Importantly, the proposed compression framework is a paradigm for addressing intricate rate-distortion optimization forms via iterative solution of easier problems emerging from the ADMM method (or other variable-splitting optimization techniques [2]). Indeed, the problem addressed here is an extension of our recent compression method [3] that pre-compensates for a later degradation occurring after decompression. In this paper the task is harder than in [3], as the source signal is available only in its degraded version. The recent wide use of ADMM for complicated signal restoration problems (e.g., [4]–[8]) suggests that our ADMM-based approach for complicated compression problems entails great potential.

Essentially, we study here a remote source coding problem (e.g., see its origins in [9], [10] and their successors). Our contribution is mainly the deterministic setting versus the statistical perspective used in previous works. Specifically, we consider an operational rate-distortion problem for the compression of a given signal, based on a different distortion metric imposed by the lack of an explicit statistical model of the unknown source. Our settings lead to the remarkable

result that, using the ADMM technique, one can employ a standard compression method to address remote source coding problems in much more complicated instances than were previously feasible (e.g., [11]).

Using rate-distortion theory, we further study the examined problem in statistical settings (considering the proposed distortion metric) for the case of a cyclo-stationary Gaussian source signal and linear shift-invariant system operators. Our results show that the initial rate-distortion optimization reduces to a reverse water-filling procedure adjusted to the system operators and considering the pseudoinverse-filtered version of the input signal. We use these theoretic results to explain concepts appearing (differently) in the proposed practical method intended for non-Gaussian signals and general linear system operators.

Jointly using sampling and source coding procedures is fundamental to digitization-based systems (see, e.g., [12]). Accordingly, we demonstrate our general framework for adapting standard compression methods to the specific settings of a complete acquisition-rendering system. We present experiments considering coding of one-dimensional signals using an adaptive tree-based technique, and to video compression using the state-of-the-art HEVC standard [13]. Comparisons of our strategy to a regular compression flow exhibited that our method achieves significant gains at medium/high bit-rates.

## II. THE PROPOSED METHOD

Let us describe the considered system structure (Fig. 1). A source signal, an  $N$ -length column vector  $\mathbf{x} \in \mathbb{R}^N$ , undergoes a linear processing represented by the  $M \times N$  matrix  $\mathbf{A}$  and, then, deteriorated by an additive white Gaussian noise vector  $\mathbf{n} \sim \mathcal{N}(0, \sigma_n^2 \mathbf{I})$ , resulting in the signal

$$\mathbf{w} = \mathbf{A}\mathbf{x} + \mathbf{n} \quad (1)$$

where  $\mathbf{w}$  and  $\mathbf{n}$  are  $M$ -length column vectors. We represent the lossy compression procedure via the mapping  $C: \mathbb{R}^M \rightarrow \mathcal{B}$  from the  $M$ -dimensional signal domain to a discrete set  $\mathcal{B}$  of binary compressed representations (that may have different lengths). The signal  $\mathbf{w}$  is the input to the compression component of the system, producing the compressed binary data  $b = C(\mathbf{w})$  that can be stored or transmitted in an error-free manner. Then, on a device and settings depending on the specific application, the compressed data  $b \in \mathcal{B}$  is decompressed to provide the signal  $\mathbf{v} = F(b)$  where  $F: \mathcal{B} \rightarrow \mathcal{S}$  represents the decompression mapping between the binary compressed representations in  $\mathcal{B}$  to the corresponding decompressed signals in the discrete set  $\mathcal{S} \subset \mathbb{R}^M$ . The decompressed signal  $\mathbf{v}$  is further processed by the linear operator denoted as the  $N \times M$  matrix  $\mathbf{B}$ , resulting in the system output signal

$$\mathbf{y} = \mathbf{B}\mathbf{v}, \quad (2)$$

which is an  $N$ -length real-valued column vector.

As an example, consider an acquisition-compression-rendering system where the signal  $\mathbf{w}$  is a sampled version of the source signal  $\mathbf{x}$ , and the system output  $\mathbf{y}$  is the rendered version of the decompressed signal  $\mathbf{v}$ .

We assume here that the operators  $\mathbf{A}$  and  $\mathbf{B}$ , as well as the noise variance  $\sigma_n^2$ , are known and fixed (i.e., cannot be optimized). Consequently, we formulate a new compression procedure in order to optimize the end-to-end rate-distortion performance of the entire system. Specifically, we want the system output  $\mathbf{y}$  to be the best approximation of the source signal  $\mathbf{x}$  under the bit-budget constraint. However, at the compression stage we do not accurately know  $\mathbf{x}$ , but rather its degraded form  $\mathbf{w}$  formulated in (1). This motivates us to suggest the following distortion metric with respect to the system output  $\mathbf{y}$

$$d_s(\mathbf{w}, \mathbf{y}) = \frac{1}{M} \|\mathbf{w} - \mathbf{A}\mathbf{y}\|_2^2. \quad (3)$$

This metric conforms with the fact that if  $\mathbf{y}$  is close to  $\mathbf{x}$ , then, by (1),  $\mathbf{w}$  will be close to  $\mathbf{A}\mathbf{y}$  up to the noise  $\mathbf{n}$ . Indeed, for the ideal case of  $\mathbf{y} = \mathbf{x}$  the metric (3) becomes

$$d_s(\mathbf{w}, \mathbf{x}) = \frac{1}{M} \|\mathbf{n}\|_2^2 \approx \sigma_n^2 \quad (4)$$

where the last approximate equality is under the assumption of a sufficiently large  $M$  (the length of  $\mathbf{n}$ ). Since  $\mathbf{y} = \mathbf{B}\mathbf{v}$ , we can rewrite the distortion  $d_s(\mathbf{w}, \mathbf{y})$  in (3) as a function of the decompressed signal  $\mathbf{v}$ , namely,

$$d_c(\mathbf{w}, \mathbf{v}) = \frac{1}{M} \|\mathbf{w} - \mathbf{A}\mathbf{B}\mathbf{v}\|_2^2. \quad (5)$$

Since the operator  $\mathbf{B}$  produces the output signal  $\mathbf{y}$ , an ideal result will be  $\mathbf{y} = \mathbf{P}_B\mathbf{x}$ , where  $\mathbf{P}_B$  is the matrix projecting onto  $\mathbf{B}$ 's range. The corresponding ideal distortion is

$$D_0 \triangleq d_s(\mathbf{w}, \mathbf{P}_B\mathbf{x}) = \frac{1}{M} \|\mathbf{A}(\mathbf{I} - \mathbf{P}_B)\mathbf{x} + \mathbf{n}\|_2^2. \quad (6)$$

We use the distortion metric (5) to constrain the bit-cost minimization in the following rate-distortion optimization

$$\begin{aligned} \hat{\mathbf{v}} &= \underset{\mathbf{v} \in \mathcal{S}}{\operatorname{argmin}} R(\mathbf{v}) \\ \text{subject to} \quad D_0 &\leq \frac{1}{M} \|\mathbf{w} - \mathbf{A}\mathbf{B}\mathbf{v}\|_2^2 \leq D_0 + D \end{aligned} \quad (7)$$

where  $R(\mathbf{v})$  evaluates the length of the binary compressed description of the decompressed signal  $\mathbf{v}$ , and  $D \geq 0$  determines the allowed distortion. By (6), the value  $D_0$  depends on the operator  $\mathbf{A}$ , the null space of  $\mathbf{B}$ , the source signal  $\mathbf{x}$ , and the noise realization  $\mathbf{n}$ . Since  $\mathbf{x}$  and  $\mathbf{n}$  are unknown,  $D_0$  cannot be accurately calculated in the operational case (in Section III we formulate the expected value of  $D_0$  for the case of a cyclo-stationary Gaussian source signal). We address the optimization (7) using its unconstrained Lagrangian form

$$\hat{\mathbf{v}} = \underset{\mathbf{v} \in \mathcal{S}}{\operatorname{argmin}} R(\mathbf{v}) + \lambda \frac{1}{M} \|\mathbf{w} - \mathbf{A}\mathbf{B}\mathbf{v}\|_2^2 \quad (8)$$

where  $\lambda \geq 0$  is a Lagrange multiplier corresponding to some distortion constraint  $D_\lambda \geq D_0$  (such optimization strategy with respect to some Lagrange multiplier is common, e.g., in video coding [13]). In the case of high-dimensional signals, the discrete set  $\mathcal{S}$  is extremely large and, therefore, it is impractical to directly solve the Lagrangian form in (8) for generally structured matrices  $\mathbf{A}$  and  $\mathbf{B}$ . This difficulty vanishes, for example,

when  $\mathbf{A} = \mathbf{B} = \mathbf{I}$ , reducing the Lagrangian optimization in (8) to the standard (system independent) compression form (see, e.g., [14], [15]). Indeed, such standard Lagrangian rate-distortion optimizations are practically solved using block-based designs that translate the task to a sequence of block-level optimizations of feasible dimensions.

Here we consider general  $\mathbf{A}$  and  $\mathbf{B}$  matrices, and address the computational difficulty in solving (8) using the alternating direction method of multipliers (ADMM) technique [1]. For start, we apply variable splitting to rewrite (8) as

$$\begin{aligned} \hat{\mathbf{v}} = \underset{\mathbf{v} \in \mathcal{S}, \mathbf{z} \in \mathbb{R}^M}{\operatorname{argmin}} \quad & R(\mathbf{v}) + \lambda \frac{1}{M} \|\mathbf{w} - \mathbf{ABz}\|_2^2 \\ \text{subject to} \quad & \mathbf{v} = \mathbf{z} \end{aligned} \quad (9)$$

where  $\mathbf{z} \in \mathbb{R}^M$  is an auxiliary variable that is not (directly) restricted to the discrete set  $\mathcal{S}$ . The augmented Lagrangian (in its scaled form) and the method of multipliers (see [1, Ch. 2]) turn (9) into the following iterative procedure

$$(\hat{\mathbf{v}}^{(t)}, \hat{\mathbf{z}}^{(t)}) = \quad (10)$$

$$\begin{aligned} \underset{\mathbf{v} \in \mathcal{S}, \mathbf{z} \in \mathbb{R}^M}{\operatorname{argmin}} \quad & R(\mathbf{v}) + \lambda \frac{1}{M} \|\mathbf{w} - \mathbf{ABz}\|_2^2 + \frac{\beta}{2} \|\mathbf{v} - \mathbf{z} + \mathbf{u}^{(t)}\|_2^2 \\ \mathbf{u}^{(t+1)} = \mathbf{u}^{(t)} + & (\hat{\mathbf{v}}^{(t)} - \hat{\mathbf{z}}^{(t)}), \end{aligned} \quad (11)$$

where  $t$  is the iteration number,  $\mathbf{u}^{(t)} \in \mathbb{R}^M$  is the scaled dual variable, and  $\beta$  is an auxiliary parameter originating at the augmented Lagrangian. Further simplifying (10) using one iteration of alternating minimization gives the ADMM form of the problem

$$\hat{\mathbf{v}}^{(t)} = \underset{\mathbf{v} \in \mathcal{S}}{\operatorname{argmin}} R(\mathbf{v}) + \frac{\beta}{2} \|\mathbf{v} - \tilde{\mathbf{z}}^{(t)}\|_2^2 \quad (12)$$

$$\hat{\mathbf{z}}^{(t)} = \underset{\mathbf{z} \in \mathbb{R}^M}{\operatorname{argmin}} \lambda \frac{1}{M} \|\mathbf{w} - \mathbf{ABz}\|_2^2 + \frac{\beta}{2} \|\mathbf{z} - \tilde{\mathbf{v}}^{(t)}\|_2^2 \quad (13)$$

$$\mathbf{u}^{(t+1)} = \mathbf{u}^{(t)} + (\hat{\mathbf{v}}^{(t)} - \hat{\mathbf{z}}^{(t)}). \quad (14)$$

where  $\tilde{\mathbf{z}}^{(t)} = \hat{\mathbf{z}}^{(t-1)} - \mathbf{u}^{(t)}$  and  $\tilde{\mathbf{v}}^{(t)} = \hat{\mathbf{v}}^{(t)} + \mathbf{u}^{(t)}$ . Importantly, the compression design, expressed by  $\{\mathcal{S}, R\}$ , and the system-specific operators  $\{\mathbf{A}, \mathbf{B}\}$  were decoupled by the ADMM to reside in distinct optimization problems that are easier to solve.

We identify the first stage (12) as the Lagrangian optimization employed for standard compression (and decompression) tasks considering the regular mean squared error metric. Specifically, the Lagrange multiplier for this standard optimization is  $\tilde{\lambda} = \frac{\beta M}{2}$ . Furthermore, we suggest to replace the solution of (12) with the application of a standard compression (and decompression) technique, even one that does not follow the Lagrangian optimization formulated in (12). We denote the standard compression and decompression via

$$b^{(t)} = \text{StandardCompress}(\tilde{\mathbf{z}}^{(t)}, \theta) \quad (15)$$

$$\hat{\mathbf{v}}^{(t)} = \text{StandardDecompress}(b^{(t)}) \quad (16)$$

where  $\theta$  is a general parameter that extends the Lagrange multiplier role in determining the rate-distortion tradeoff (see

Algorithm 1). This important suggestion defines our method as a generic approach that can optimize any compression technique with respect to the specific system it resides in.

The second optimization stage (13) is an  $\ell_2$ -constrained deconvolution problem, that can be easily solved in various ways. The analytic solution of (13) is

$$\hat{\mathbf{z}}^{(t)} = \left( \mathbf{B}^* \mathbf{A}^* \mathbf{AB} + \frac{\beta M}{2\lambda} \mathbf{I} \right)^{-1} \left( \mathbf{B}^* \mathbf{A}^* \mathbf{w} + \frac{\beta M}{2\lambda} \tilde{\mathbf{v}}^{(t)} \right) \quad (17)$$

showing it as a weighted averaging of  $\mathbf{w}$  and  $\tilde{\mathbf{v}}^{(t)}$ . In the generic description given in Algorithm 1 we replace the quantity  $\frac{\beta M}{2\lambda}$  with the parameter  $\beta$ .

The proposed method is summarized in Algorithm 1. Our goal is to provide a binary compressed representation of the optimized solution. Hence, the procedure output is the compressed data,  $b^{(t)}$ , obtained in the compression stage of the last iteration.

---

#### Algorithm 1 Generic System-Aware Compression

---

- 1: Inputs:  $\mathbf{w}$ ,  $\theta$ ,  $\tilde{\beta}$ .
  - 2: Initialize  $t = 0$ ,  $\hat{\mathbf{z}}^{(0)} = \mathbf{w}$ ,  $\mathbf{u}^{(1)} = \mathbf{0}$ .
  - 3: **repeat**
  - 4:    $t \leftarrow t + 1$
  - 5:    $\tilde{\mathbf{z}}^{(t)} = \hat{\mathbf{z}}^{(t-1)} - \mathbf{u}^{(t)}$
  - 6:    $b^{(t)} = \text{StandardCompress}(\tilde{\mathbf{z}}^{(t)}, \theta)$
  - 7:    $\hat{\mathbf{v}}^{(t)} = \text{StandardDecompress}(b^{(t)})$
  - 8:    $\tilde{\mathbf{v}}^{(t)} = \hat{\mathbf{v}}^{(t)} + \mathbf{u}^{(t)}$
  - 9:    $\hat{\mathbf{z}}^{(t)} = \left( \mathbf{B}^* \mathbf{A}^* \mathbf{AB} + \tilde{\beta} \mathbf{I} \right)^{-1} \left( \mathbf{B}^* \mathbf{A}^* \mathbf{w} + \tilde{\beta} \tilde{\mathbf{v}}^{(t)} \right)$
  - 10:    $\mathbf{u}^{(t+1)} = \mathbf{u}^{(t)} + (\hat{\mathbf{v}}^{(t)} - \hat{\mathbf{z}}^{(t)})$
  - 11: **until** stopping criterion is satisfied
  - 12: Output:  $b^{(t)}$ , which is the binary compressed data obtained in the last iteration.
- 

### III. THEORETIC ANALYSIS FOR THE GAUSSIAN CASE

In this section we use the rate-distortion theory framework to further explore the fundamental problem of system-optimized compression. We consider the case of a cyclostationary Gaussian signal and system involving linear shift-invariant operators and no noise, yet, the obtained results exhibit the prominent ideas of the general problem and the operational method presented in Section II.

#### A. Problem Formulation and Solution

The source signal is modeled here as  $\mathbf{x} \sim \mathcal{N}(0, \mathbf{R}_{\mathbf{x}})$ , i.e., a zero-mean Gaussian random vector with a circulant autocorrelation matrix  $\mathbf{R}_{\mathbf{x}}$ . The eigenvalues of  $\mathbf{R}_{\mathbf{x}}$  are denoted as  $\{\lambda_k^{(\mathbf{x})}\}_{k=0}^{N-1}$ . The first processing part of the system produces the signal  $\mathbf{w} = \mathbf{Ax}$ , where here  $\mathbf{A}$  is a real-valued  $N \times N$  circulant matrix. Evidently, the signal  $\mathbf{w}$  is a zero-mean Gaussian random vector with autocorrelation matrix  $\mathbf{R}_{\mathbf{w}} = \mathbf{AR}_{\mathbf{x}}\mathbf{A}^*$ .

Here  $\mathbf{A}$  and  $\mathbf{B}$  are circulant  $N \times N$  matrices, thus, diagonalized by the  $N \times N$  Discrete Fourier Transform (DFT)

matrix  $\mathbf{F}$  as  $\mathbf{F}\mathbf{A}\mathbf{F}^* = \mathbf{\Lambda}_\mathbf{A}$  and  $\mathbf{F}\mathbf{B}\mathbf{F}^* = \mathbf{\Lambda}_\mathbf{B}$ , where  $\mathbf{\Lambda}_\mathbf{A}$  and  $\mathbf{\Lambda}_\mathbf{B}$  are diagonal matrices formed by the elements  $\{a_k^F\}_{k=0}^{N-1}$  and  $\{b_k^F\}_{k=0}^{N-1}$ , respectively. Accordingly, the pseudoinverse matrix of  $\mathbf{A}$  is defined as  $\mathbf{A}^+ = \mathbf{F}^* \mathbf{\Lambda}_\mathbf{A}^+ \mathbf{F}$ , where  $\mathbf{\Lambda}_\mathbf{A}^+$  is the pseudoinverse of  $\mathbf{\Lambda}_\mathbf{A}$ , an  $N \times N$  diagonal matrix with the  $k^{th}$  diagonal component  $a_k^{F,+} = 1/a_k^F$  for  $k$  where  $a_k^F \neq 0$ , and  $a_k^{F,+} = 0$  for  $k$  where  $a_k^F = 0$ . The matrix  $\mathbf{B}$  has corresponding definitions to those given above for  $\mathbf{A}$ .

Recall that the system output is  $\mathbf{y} = \mathbf{B}\mathbf{v}$ , where here  $\mathbf{v}$  is the random vector representing the decompressed signal. Accordingly, in the theoretic framework here, the rate is associated with the mutual information  $I(\mathbf{w}, \mathbf{y})$ . In (7) we formulated the operational rate-distortion optimization describing our practical task, cast here in the theoretic framework to

$$\begin{aligned} \min_{p_{\mathbf{v}|\mathbf{w}}} \quad & I(\mathbf{w}; \mathbf{B}\mathbf{v}) \\ \text{s.t.} \quad & NE\{D_0\} \leq E\left\{\|\mathbf{w} - \mathbf{A}\mathbf{B}\mathbf{v}\|_2^2\right\} \leq N(E\{D_0\} + D) \end{aligned} \quad (18)$$

where  $p_{\mathbf{v}|\mathbf{w}}$  is the conditional probability-density-function of  $\mathbf{v}$  given  $\mathbf{w}$ , and  $D \geq 0$  determines the allowed expected distortion. The value  $E\{D_0\}$ , stemming from (6) and the noiseless settings here, is the minimal expected distortion evaluated (see Appendix A) as

$$E\{D_0\} = \frac{1}{N} \sum_{k: a_k^F \neq 0, b_k^F = 0} |a_k^F|^2 \lambda_k^{(\mathbf{x})}. \quad (19)$$

We state that the basic rate-distortion optimization problem in (18) is equivalent to (see proof in Appendix B)

$$\begin{aligned} \min_{p_{\mathbf{v}|\tilde{\mathbf{w}}}} \quad & I(\tilde{\mathbf{w}}; \mathbf{P}_\mathbf{B} \mathbf{P}_\mathbf{A} \mathbf{v}) \\ \text{s.t.} \quad & E\left\{\|\mathbf{A}\mathbf{B}(\tilde{\mathbf{w}} - \mathbf{v})\|_2^2\right\} \leq ND \end{aligned} \quad (20)$$

where  $\tilde{\mathbf{w}} = \mathbf{B}^+ \mathbf{A}^+ \mathbf{w}$  is the pseudoinverse filtered compression-input  $\mathbf{w}$ . Here  $\mathbf{P}_\mathbf{A}$  and  $\mathbf{P}_\mathbf{B}$  are projection matrices corresponding to the range of  $\mathbf{A}$  and  $\mathbf{B}$ , respectively. We define the set  $\mathcal{K}_{AB} \triangleq \{k : a_k^F \neq 0 \text{ and } b_k^F \neq 0\}$  that contains the DFT-domain component indices belonging to the range of the joint operator  $\mathbf{AB}$ .

Since  $\tilde{\mathbf{w}}$  is a cyclo-stationary Gaussian random vector, we transform the optimization (20) into a Fourier-domain distortion-allocation problem considering independent Gaussian variables (see proof in Appendix C), namely,

$$\begin{aligned} \min_{\{D_k\}_{k \in \mathcal{K}_{AB}}} \quad & \sum_{k \in \mathcal{K}_{AB}} \frac{1}{2} \log \left( \frac{\lambda_k^{(\tilde{\mathbf{w}})}}{D_k} \right) \\ \text{s.t.} \quad & \sum_{k \in \mathcal{K}_{AB}} |a_k^F b_k^F|^2 D_k \leq ND \\ & 0 \leq D_k \leq \lambda_k^{(\tilde{\mathbf{w}})}, \quad k \in \mathcal{K}_{AB}. \end{aligned} \quad (21)$$

where for  $k \in \mathcal{K}_{AB}$  the value  $\lambda_k^{(\tilde{\mathbf{w}})} = \lambda_k^{(\mathbf{w})} / |a_k^F b_k^F|^2$  is the variance of the  $k^{th}$  DFT-coefficient of  $\tilde{\mathbf{w}}$ . The solution of problem (21), obtained using Lagrangian optimization and

the KKT conditions, is given by the following distortion allocation: for  $k \in \mathcal{K}_{AB}$

$$D_k = \begin{cases} \theta / |a_k^F b_k^F|^2, & \text{for } 0 \leq \theta < |a_k^F b_k^F|^2 \lambda_k^{(\tilde{\mathbf{w}})} \\ \lambda_k^{(\tilde{\mathbf{w}})}, & \text{for } \theta \geq |a_k^F b_k^F|^2 \lambda_k^{(\tilde{\mathbf{w}})}, \end{cases} \quad (22)$$

where  $\theta$  is set such that  $\sum_{k \in \mathcal{K}_{AB}} |a_k^F b_k^F|^2 D_k = ND$  is satisfied.

Importantly, for  $k \notin \mathcal{K}_{AB}$  the rate is  $R_k = 0$  and the distortion is set to  $D_k = 0$  (see Appendix C). The optimal rates corresponding to (22) assign for  $k \in \mathcal{K}_{AB}$  that also obeys  $0 \leq \theta < |a_k^F b_k^F|^2 \lambda_k^{(\tilde{\mathbf{w}})}$

$$R_k = \frac{1}{2} \log \left( |a_k^F b_k^F|^2 \frac{\lambda_k^{(\tilde{\mathbf{w}})}}{\theta} \right) \quad (23)$$

and otherwise  $R_k = 0$ . Eq. (23) shows that the optimal rate assignments include compensation for the modulation applied beforehand in the pseudoinverse filtering of the input  $\mathbf{w}$ . Moreover, DFT components belonging to the null spaces of  $\mathbf{A}$  and  $\mathbf{B}$  are not coded (i.e., get zero rates).

### B. Problem Solution in Theory and Practice

While the theoretic framework above considers a cyclo-stationary Gaussian signal and a noiseless system composed of linear shift-invariant operators, the solution presented exhibits important ideas that also appear in the practical method of Section II. Recall that our method is designed for the operational settings of the problem treating non-Gaussian signals and general linear operators, hence, the resemblances between the above theory and practice are at the conceptual level and may materialize differently.

We addressed the theoretic problem (18) using a simple inverse filtering of the input data  $\mathbf{w}$ , transforming the problem into (20) and (21) that were solved using an extended version of the standard reverse water-filling procedure. Analogously, our practical method (Algorithm 1) repeatedly compresses a signal formed by an  $\ell_2$ -constrained deconvolution filtering, that can be rewritten also as a pseudoinverse filtering of the input followed by a weighted averaging with  $\tilde{\mathbf{v}}^{(t)}$ , i.e.,

$$\hat{\mathbf{z}}^{(t)} = \left( \mathbf{B}^* \mathbf{A}^* \mathbf{AB} + \tilde{\beta} \mathbf{I} \right)^{-1} \left( \mathbf{B}^* \mathbf{A}^* \mathbf{AB} \tilde{\mathbf{w}} + \tilde{\beta} \tilde{\mathbf{v}}^{(t)} \right). \quad (24)$$

This shows that, in practice as well as in theory, the input  $\mathbf{w}$  should go through a pseudoinverse filtering (softened via (24)) as a preceding stage to compression.

The second prominent principle of the theoretic solution, exhibited in (23), is to compensate for the modulation applied by the pseudoinverse filter corresponding to the effective system operator  $\mathbf{AB}$ . Similarly in Algorithm 1, the constrained deconvolution stage (24) implements this idea by better preserving  $\tilde{\mathbf{w}}$  components corresponding to higher energy parts of  $\mathbf{AB}$ . This is clearly observed in the particular case of circulant  $\mathbf{A}$  and  $\mathbf{B}$ , where the filtering (24) reduces to the DFT-domain component-level operation of

$$\hat{z}_k^{F,(t)} = \left( |a_k^F b_k^F|^2 \tilde{w}_k^F + \tilde{\beta} \tilde{v}_k^{F,(t)} \right) / \left( |a_k^F b_k^F|^2 + \tilde{\beta} \right) \quad (25)$$

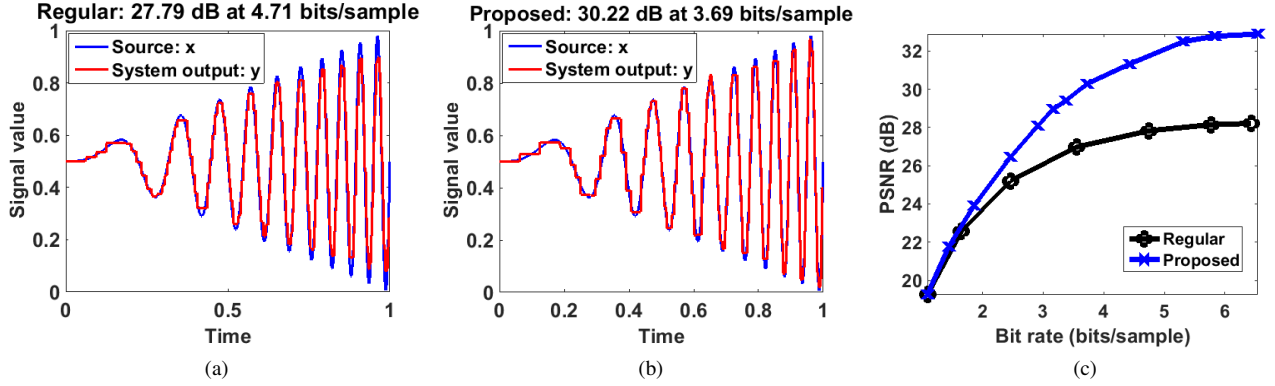


Fig. 2. Experiment for one-dimensional signal and adaptive tree-based coding in an acquisition-rendering system. The amplitude-modulated chirp source signal is the blue curve in (a) and (b). The red curves in (a) and (b) are the system output (rendered) signals resulting from regular compression and the proposed method, respectively. (c) Comparison of PSNR-bitrate curves.

where  $\tilde{w}_k^F$  and  $\tilde{v}_k^{F,(t)}$  are the  $k^{th}$  DFT-coefficients of  $\tilde{\mathbf{w}}$  and  $\tilde{\mathbf{v}}^{(t)}$ , respectively.

#### IV. EXPERIMENTAL RESULTS

In this section we employ Algorithm 1 to adjust standard compression designs to acquisition-rendering systems where the compression is an intermediate stage. Specifically, we model the source as a high-resolution discrete signal, acquired via linear shift-invariant low-pass filtering and uniform sub-sampling. Then, this acquired signal is available for compression, and after decompression it is linearly rendered back to the source resolution by replicating each decompressed sample (in a uniform pattern matching the source sub-sampling).

1) *Coding of One Dimensional Signals:* The compression approach here relies on adaptive tree-based segmentation of the signal (for another instance of this prevalent idea see [16]). Specifically, here we compress a one-dimensional signal using an operational rate-distortion optimization determining a binary-tree corresponding to a non-uniform segmentation of the signal, where each segment is represented by a constant value defined by the quantized average-value of the interval (see more details in Appendix D). We consider the system flow of acquisition-compression-decompression-rendering for an amplitude-modulated chirp source signal. Figures 2a and 2b exhibit the system output (i.e., the rendered signal) resulting from the use of a regular compression at 4.71 bpp and from employing our method at 3.69 bpp, respectively. Evidently, our method outperforms the regular approach in terms of PSNR and also in reproducing the chirp signal peaks. Comparing our method to the regular approach at various bit-rates (Fig. 2c) shows significant PSNR gains at medium/high bit-rates.

2) *Video Coding:* We evaluated our method also for adjusting the HEVC coding standard [13] to a simplified acquisition-rendering system, considering the spatial dimensions of the frames (more details are provided in Appendix E). The PSNR-bitrate curves in Fig. 3 and the visual results (see Appendix E) show the capability of our approach for generically adapting a complicated compression method to a given system structure.

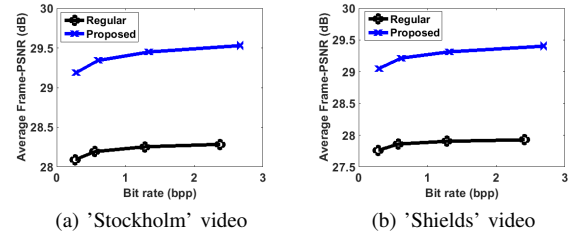


Fig. 3. HEVC coding of 10 video frames. The curves present the PSNR of the system rendered output with respect to the high-resolution source.

#### V. CONCLUSION

In this paper we considered a system employing lossy compression as an intermediate stage, and proposed a methodology to optimize the system rate-distortion performance from the compression standpoint. We presented a generic operational method and explained its main ideas using rate-distortion theory of Gaussian signals. We provided experimental demonstrations of the effectiveness of our approach for coding of 1D signals and video sequences.

#### ACKNOWLEDGMENT

This research was supported in part by the European Research Council under European Unions Seventh Framework Program, ERC Grant agreement no. 320649, and by the Israel Science Foundation grant no. 2597/16.

#### REFERENCES

- [1] S. Boyd, N. Parikh, E. Chu, B. Peleato, and J. Eckstein, "Distributed optimization and statistical learning via the alternating direction method of multipliers," *Foundations and Trends in Machine Learning*, vol. 3, no. 1, pp. 1–122, 2011.
- [2] Y. Dar, M. Elad, and A. M. Bruckstein, "Restoration by compression," *arXiv preprint arXiv:1711.05147*, 2017.
- [3] —, "Optimized pre-compensating compression," *arXiv preprint arXiv:1711.07901*, 2017.
- [4] M. V. Afonso, J. M. Bioucas-Dias, and M. A. Figueiredo, "Fast image recovery using variable splitting and constrained optimization," *IEEE Trans. Image Process.*, vol. 19, no. 9, pp. 2345–2356, 2010.
- [5] S. V. Venkatakrishnan, C. A. Bouman, and B. Wohlberg, "Plug-and-play priors for model based reconstruction," in *IEEE GlobalSIP*, 2013.

- [6] Y. Dar, A. M. Bruckstein, M. Elad, and R. Giryes, "Postprocessing of compressed images via sequential denoising," *IEEE Trans. Image Process.*, vol. 25, no. 7, pp. 3044–3058, 2016.
- [7] A. Rond, R. Giryes, and M. Elad, "Poisson inverse problems by the plug-and-play scheme," *Journal of Visual Communication and Image Representation*, vol. 41, pp. 96–108, 2016.
- [8] Y. Romano, M. Elad, and P. Milanfar, "The little engine that could: Regularization by denoising (red)," *SIAM Journal on Imaging Sciences*, vol. 10, no. 4, pp. 1804–1844, 2017.
- [9] R. Dobrushin and B. Tsybakov, "Information transmission with additional noise," *IRE Trans. Inf. Theory*, vol. 8, no. 5, pp. 293–304, 1962.
- [10] J. Wolf and J. Ziv, "Transmission of noisy information to a noisy receiver with minimum distortion," *IEEE Trans. Inf. Theory*, vol. 16, no. 4, pp. 406–411, 1970.
- [11] O. K. Al-Shaykh and R. M. Mersereau, "Lossy compression of noisy images," *IEEE Trans. Image Process.*, vol. 7, no. 12, pp. 1641–1652, 1998.
- [12] A. Kipnis, A. J. Goldsmith, Y. C. Eldar, and T. Weissman, "Distortion rate function of sub-Nyquist sampled Gaussian sources," *IEEE Trans. Inf. Theory*, vol. 62, no. 1, pp. 401–429, 2016.
- [13] G. J. Sullivan, J. Ohm, W.-J. Han, and T. Wiegand, "Overview of the high efficiency video coding (hevc) standard," *IEEE Trans. Circuits and Systems for Video Technology*, vol. 22, no. 12, pp. 1649–1668, 2012.
- [14] Y. Shoham and A. Gersho, "Efficient bit allocation for an arbitrary set of quantizers," *IEEE Trans. Acoust., Speech, Signal Process.*, vol. 36, no. 9, pp. 1445–1453, 1988.
- [15] A. Ortega and K. Ramchandran, "Rate-distortion methods for image and video compression," *IEEE Signal Process. Mag.*, vol. 15, no. 6, pp. 23–50, 1998.
- [16] R. Shukla, P. L. Dragotti, M. N. Do, and M. Vetterli, "Rate-distortion optimized tree-structured compression algorithms for piecewise polynomial images," *IEEE Trans. Image Process.*, vol. 14, no. 3, pp. 343–359, 2005.
- [17] P. A. Chou, T. Lookabaugh, and R. M. Gray, "Optimal pruning with applications to tree-structured source coding and modeling," *IEEE Trans. Inf. Theory*, vol. 35, no. 2, pp. 299–315, 1989.
- [18] H. Everett III, "Generalized lagrange multiplier method for solving problems of optimum allocation of resources," *Operations research*, vol. 11, no. 3, pp. 399–417, 1963.

#### APPENDIX A

##### THE THEORETIC SETTINGS: MINIMAL EXPECTED DISTORTION

The minimal distortion was defined in (6) for the operational settings. Here we will formulate its expected value, needed for the statistical settings of Section III. Expecting (6), considering  $M = N$  and no noise, gives

$$\begin{aligned}
 E\{D_0\} &= \frac{1}{N} E \left\{ \|\mathbf{A}(\mathbf{I} - \mathbf{P}_B) \mathbf{x}\|_2^2 \right\} \\
 &= \frac{1}{N} E \left\{ \|\mathbf{F}^* \mathbf{\Lambda}_A \mathbf{F} \mathbf{F}^* (\mathbf{I} - \mathbf{\Lambda}_{P_B}) \mathbf{F} \mathbf{x}\|_2^2 \right\} \\
 &= \frac{1}{N} E \left\{ \|\mathbf{\Lambda}_A (\mathbf{I} - \mathbf{\Lambda}_{P_B}) \mathbf{x}^F\|_2^2 \right\} \\
 &= \frac{1}{N} E \left\{ \sum_{k: a_k^F \neq 0, b_k^F = 0} |a_k^F x_k^F|^2 \right\} \\
 &= \frac{1}{N} \sum_{k: a_k^F \neq 0, b_k^F = 0} |a_k^F|^2 \lambda_k^{(\mathbf{x})}, \quad (26)
 \end{aligned}$$

where  $\mathbf{x}^F \triangleq \mathbf{F} \mathbf{x}$ . Furthermore, we used the circulant structure of  $\mathbf{P}_B$  (as it is the projection matrix corresponding to the range of the circulant matrix  $\mathbf{B}$ ) providing the DFT-based diagonalization via  $\mathbf{F} \mathbf{P}_B \mathbf{F}^* = \mathbf{\Lambda}_{P_B}$ . Moreover, we utilized the formation of the diagonal matrix  $\mathbf{\Lambda}_{P_B}$  where the  $(k, k)$

entry is 1 for  $k$  corresponding to  $b_k^F \neq 0$ , and otherwise the  $(k, k)$  entry is 0.

#### APPENDIX B

##### THE THEORETIC SETTINGS: EQUIVALENCE OF OPTIMIZATION PROBLEMS (18) AND (20)

Let us begin by proving the equivalence between the distortion constraints of optimizations (18) and (20). We define the matrix  $\mathbf{H} \triangleq \mathbf{A} \mathbf{B}$  joining the two linear operators of the system. In Section III we considered  $\mathbf{A}$  and  $\mathbf{B}$  to be  $N \times N$  circulant matrices and, thus,  $\mathbf{H}$  is also a  $N \times N$  circulant matrix. Consequently,  $\mathbf{H}$  is diagonalized by the  $N \times N$  DFT matrix  $\mathbf{F}$  via  $\mathbf{F} \mathbf{H} \mathbf{F}^* = \mathbf{\Lambda}_H$ , where  $\mathbf{\Lambda}_H$  is a diagonal matrix formed by the elements  $h_k^F = a_k^F b_k^F$  for  $k = 0, \dots, N-1$ . The pseudoinverse matrix of  $\mathbf{H}$  is defined as  $\mathbf{H}^+ = \mathbf{F}^* \mathbf{\Lambda}_H^+ \mathbf{F}$ , where  $\mathbf{\Lambda}_H^+$  is the pseudoinverse of  $\mathbf{\Lambda}_H$ , an  $N \times N$  diagonal matrix with the  $k^{th}$  diagonal component

$$h_k^{F,+} = \begin{cases} \frac{1}{a_k^F b_k^F} & , \text{for } k \in \mathcal{K}_{AB} \\ 0 & , \text{for } k \notin \mathcal{K}_{AB}. \end{cases} \quad (27)$$

where  $\mathcal{K}_{AB} \triangleq \{k : a_k^F \neq 0 \text{ and } b_k^F \neq 0\}$  includes the DFT-domain component indices defining the range of the joint operator  $\mathbf{A} \mathbf{B}$ .

Now, let us develop the distortion expression appearing in the constraint of optimization (18):

$$\begin{aligned}
 \|\mathbf{w} - \mathbf{A} \mathbf{B} \mathbf{v}\|_2^2 &= \|\mathbf{w} - \mathbf{H} \mathbf{v}\|_2^2 \\
 &= \|(\mathbf{I} - \mathbf{H} \mathbf{H}^+) \mathbf{w} + \mathbf{H} \mathbf{H}^+ \mathbf{w} - \mathbf{H} \mathbf{v}\|_2^2 \\
 &= \|(\mathbf{I} - \mathbf{H} \mathbf{H}^+) \mathbf{w} + \mathbf{H} (\mathbf{H}^+ \mathbf{w} - \mathbf{v})\|_2^2 \\
 &= \|(\mathbf{I} - \mathbf{H} \mathbf{H}^+) \mathbf{w}\|_2^2 + \|\mathbf{H} (\mathbf{H}^+ \mathbf{w} - \mathbf{v})\|_2^2 \\
 &\quad + (\mathbf{H}^+ \mathbf{w} - \mathbf{v})^* \mathbf{H}^* (\mathbf{I} - \mathbf{H} \mathbf{H}^+) \mathbf{w} \\
 &\quad + \mathbf{w}^* (\mathbf{I} - \mathbf{H} \mathbf{H}^+)^* \mathbf{H} (\mathbf{H}^+ \mathbf{w} - \mathbf{v}) \\
 &= \|(\mathbf{I} - \mathbf{H} \mathbf{H}^+) \mathbf{w}\|_2^2 + \|\mathbf{H} (\mathbf{H}^+ \mathbf{w} - \mathbf{v})\|_2^2 \quad (28)
 \end{aligned}$$

where the last equality readily stems from the relation

$$\mathbf{H}^* (\mathbf{I} - \mathbf{H} \mathbf{H}^+) = \mathbf{0}. \quad (29)$$

We use the DFT-based diagonalization of  $\mathbf{H}$  to continue developing the expression of the first term in (28):

$$\begin{aligned}
 \|(\mathbf{I} - \mathbf{H} \mathbf{H}^+) \mathbf{w}\|_2^2 &= \|(\mathbf{I} - \mathbf{F}^* \mathbf{\Lambda}_H \mathbf{F} \mathbf{F}^* \mathbf{\Lambda}_H^+ \mathbf{F}) \mathbf{w}\|_2^2 \\
 &= \|\mathbf{F}^* (\mathbf{I} - \mathbf{\Lambda}_H \mathbf{\Lambda}_H^+) \mathbf{F} \mathbf{w}\|_2^2 \\
 &= \|(\mathbf{I} - \mathbf{\Lambda}_H \mathbf{\Lambda}_H^+) \mathbf{w}^F\|_2^2 \\
 &= \sum_{k: h_k^F = 0} |w_k^F|^2 = \\
 &= \sum_{k: a_k^F \neq 0, b_k^F = 0} |a_k^F x_k^F|^2 \quad (30)
 \end{aligned}$$

where we used the DFT-domain expression of the  $k^{th}$  component of  $\mathbf{w}^F$  as  $w_k^F = a_k^F x_k^F$ , reducing to  $w_k^F = 0$  when

$a_k^F = 0$ . Taking the expectation of (30), noting that the source signal  $\mathbf{x}$  and the noise  $\mathbf{n}$  are independent, yields

$$E \left\{ \left\| (\mathbf{I} - \mathbf{H}\mathbf{H}^+) \mathbf{w} \right\|_2^2 \right\} = \sum_{k: a_k^F \neq 0, b_k^F = 0} |a_k^F|^2 \lambda_k^{(\mathbf{x})}. \quad (31)$$

Then, using (28) and (31) we get that

$$E \left\{ \left\| \mathbf{w} - \mathbf{A}\mathbf{B}\mathbf{v} \right\|_2^2 \right\} = E \left\{ \left\| \mathbf{A}\mathbf{B}(\tilde{\mathbf{w}} - \mathbf{v}) \right\|_2^2 \right\} + \sum_{k: a_k^F \neq 0, b_k^F = 0} |a_k^F|^2 \lambda_k^{(\mathbf{x})}, \quad (32)$$

where  $\tilde{\mathbf{w}} = \mathbf{B}^+ \mathbf{A}^+ \mathbf{w}$ . Eq. (26) implies

$$NE \{D_0\} = \sum_{k: a_k^F \neq 0, b_k^F = 0} |a_k^F|^2 \lambda_k^{(\mathbf{x})} \quad (33)$$

that jointly with (32) yields the transformation of the expected distortion constraint in the optimization (18), namely,

$$NE \{D_0\} \leq E \left\{ \left\| \mathbf{w} - \mathbf{A}\mathbf{B}\mathbf{v} \right\|_2^2 \right\} \leq N (E \{D_0\} + D) \quad (34)$$

into

$$0 \leq E \left\{ \left\| \mathbf{A}\mathbf{B}(\tilde{\mathbf{w}} - \mathbf{v}) \right\|_2^2 \right\} \leq ND. \quad (35)$$

Since (35) is the distortion constraint in optimization (20), we proved that the distortion constraints of optimizations (18) and (20) are interchangeable.

We continue by showing the equivalence of the mutual information terms appearing in the optimization costs of (18) and (20). We start with  $I(\mathbf{w}; \mathbf{B}\mathbf{v})$  used in (18). By the data processing inequality, the compression-input  $\mathbf{w}$  and its filtered version  $\mathbf{A}^+ \mathbf{w}$  obey

$$I(\mathbf{w}; \mathbf{B}\mathbf{v}) \geq I(\mathbf{A}^+ \mathbf{w}; \mathbf{B}\mathbf{v}). \quad (36)$$

In the theoretic settings we consider the noiseless case where  $\mathbf{w} = \mathbf{A}\mathbf{x}$ , hence,  $\mathbf{A}^+ \mathbf{w} = \mathbf{P}_\mathbf{A} \mathbf{x}$ . Recall that  $\mathbf{P}_\mathbf{A}$  is the projection matrix of the range of  $\mathbf{A}$ . Since  $\mathbf{A}$  is circulant,  $\mathbf{P}_\mathbf{A}$  is also circulant and diagonalized by the DFT matrix via  $\mathbf{F}\mathbf{P}_\mathbf{A}\mathbf{F}^* = \mathbf{\Lambda}_{\mathbf{P}_\mathbf{A}}$  where  $\mathbf{\Lambda}_{\mathbf{P}_\mathbf{A}} = \mathbf{\Lambda}_\mathbf{A} \mathbf{\Lambda}_\mathbf{A}^+$ . Accordingly, we can write

$$\mathbf{A}\mathbf{A}^+ \mathbf{w} = \mathbf{A}\mathbf{P}_\mathbf{A} \mathbf{x} = \mathbf{A}\mathbf{x} = \mathbf{w} \quad (37)$$

exhibiting  $\mathbf{w}$  as a processing of  $\mathbf{A}^+ \mathbf{w}$ , thus, by the data processing inequality we get

$$I(\mathbf{w}; \mathbf{B}\mathbf{v}) \leq I(\mathbf{A}^+ \mathbf{w}; \mathbf{B}\mathbf{v}) \quad (38)$$

that together with (36) implies

$$I(\mathbf{w}; \mathbf{B}\mathbf{v}) = I(\mathbf{A}^+ \mathbf{w}; \mathbf{B}\mathbf{v}). \quad (39)$$

The above showed that since  $\mathbf{w}$  is in the range of  $\mathbf{A}$ , its processing via  $\mathbf{A}^+$  is invertible and, thus, the mutual information is preserved under such processing of  $\mathbf{w}$ .

Similar to the above arguments, we can show that since the system output  $\mathbf{B}\mathbf{v}$  is in the range of  $\mathbf{B}$ , its processing via  $\mathbf{B}^+$

is invertible and, therefore, the mutual information is preserved under such filtering of  $\mathbf{B}\mathbf{v}$ :

$$\begin{aligned} I(\mathbf{A}^+ \mathbf{w}; \mathbf{B}\mathbf{v}) &= I(\mathbf{A}^+ \mathbf{w}; \mathbf{B}^+ \mathbf{B}\mathbf{v}) \\ &= I(\mathbf{A}^+ \mathbf{w}; \mathbf{P}_\mathbf{B} \mathbf{v}). \end{aligned} \quad (40)$$

Consider the decomposition of  $\mathbf{A}^+ \mathbf{w}$  based on its projections on  $\mathbf{B}$ 's range and nullspace, namely,

$$\mathbf{A}^+ \mathbf{w} = \mathbf{P}_\mathbf{B} \mathbf{A}^+ \mathbf{w} + (\mathbf{I} - \mathbf{P}_\mathbf{B}) \mathbf{A}^+ \mathbf{w}. \quad (41)$$

Observe that

$$\begin{aligned} (\mathbf{I} - \mathbf{P}_\mathbf{B}) \mathbf{A}^+ \mathbf{w} &= \mathbf{F}^* (\mathbf{I} - \mathbf{\Lambda}_{\mathbf{P}_\mathbf{B}}) \mathbf{F} \mathbf{F}^* \mathbf{\Lambda}_\mathbf{A}^+ \mathbf{F} \mathbf{w} \\ &= \mathbf{F}^* (\mathbf{I} - \mathbf{\Lambda}_{\mathbf{P}_\mathbf{B}}) \mathbf{\Lambda}_\mathbf{A}^+ \mathbf{w}^F \end{aligned} \quad (42)$$

and the second random variable considered by the mutual information in (40) is

$$\begin{aligned} \mathbf{P}_\mathbf{B} \mathbf{v} &= \mathbf{F}^* \mathbf{\Lambda}_{\mathbf{P}_\mathbf{B}} \mathbf{F} \mathbf{v} \\ &= \mathbf{F}^* \mathbf{\Lambda}_{\mathbf{P}_\mathbf{B}} \mathbf{w}^F \end{aligned} \quad (43)$$

where  $\mathbf{w}^F$  is the DFT-domain representation of  $\mathbf{w}$ . Note that the diagonal projection matrices  $\mathbf{\Lambda}_{\mathbf{P}_\mathbf{B}} \triangleq \mathbf{\Lambda}_\mathbf{B} \mathbf{\Lambda}_\mathbf{B}^+$  and  $\mathbf{I} - \mathbf{\Lambda}_{\mathbf{P}_\mathbf{B}}$  appearing in (43) and (42), respectively, imply that the DFT-domain representations of  $(\mathbf{I} - \mathbf{P}_\mathbf{B}) \mathbf{A}^+ \mathbf{w}$  and  $\mathbf{P}_\mathbf{B} \mathbf{v}$  have complementary non-overlapping supports (defined by the component indices where the value may be nonzero). Let us develop the mutual information in (40) to leverage the mentioned structures and the decomposition (41):

$$\begin{aligned} I(\mathbf{A}^+ \mathbf{w}; \mathbf{P}_\mathbf{B} \mathbf{v}) &= \\ &= I(\mathbf{F} \mathbf{A}^+ \mathbf{w}; \mathbf{F} \mathbf{P}_\mathbf{B} \mathbf{v}) \end{aligned} \quad (44)$$

$$= I(\mathbf{\Lambda}_\mathbf{A}^+ \mathbf{w}^F; \mathbf{\Lambda}_{\mathbf{P}_\mathbf{B}} \mathbf{v}^F) \quad (45)$$

$$\geq \sum_{k: b_k^F \neq 0} I(a_k^{F,+} w_k^F; v_k^F) + \sum_{k: b_k^F = 0} I(a_k^{F,+} w_k^F; 0) \quad (46)$$

$$= \sum_{k: b_k^F \neq 0} I(a_k^{F,+} w_k^F; v_k^F) \quad (47)$$

where (44) is due to the preservation of mutual information under a unitary transformation. The lower bound in (46) emerges from the independence of the DFT-domain variables  $w_k^F$ ,  $k = 0, \dots, N-1$ , since they originate in the cyclostationary Gaussian signal  $\mathbf{x}$  processed by the circulant matrix  $\mathbf{A}$ . In Appendix C we exhibit a backward channel construction based on independent components  $v_k^F$  in the DFT domain, therefore, satisfying the inequality (46) with equality. Using (47) and pending on the construction shown in Appendix C, we state that

$$\begin{aligned} I(\mathbf{A}^+ \mathbf{w}; \mathbf{P}_\mathbf{B} \mathbf{v}) &= \sum_{k: b_k^F \neq 0} I(a_k^{F,+} w_k^F; v_k^F) \\ &= I(\mathbf{P}_\mathbf{B} \mathbf{A}^+ \mathbf{w}; \mathbf{P}_\mathbf{B} \mathbf{v}) \end{aligned} \quad (48)$$

Note that  $\mathbf{P}_\mathbf{B} \mathbf{A}^+ \mathbf{w}$  is in the range of  $\mathbf{A}$ , hence, using similar arguments to those given in the last paragraph, one can show that

$$I(\mathbf{P}_\mathbf{B} \mathbf{A}^+ \mathbf{w}; \mathbf{P}_\mathbf{B} \mathbf{v}) = I(\mathbf{P}_\mathbf{B} \mathbf{A}^+ \mathbf{w}; \mathbf{P}_\mathbf{A} \mathbf{P}_\mathbf{B} \mathbf{v}) \quad (49)$$

Furthermore, since  $\mathbf{P}_B \mathbf{A}^+ \mathbf{w}$  belongs also to the range of  $\mathbf{B}$ , its processing via  $\mathbf{B}^+$  is invertible, thus,

$$I(\mathbf{P}_B \mathbf{A}^+ \mathbf{w}; \mathbf{P}_A \mathbf{P}_B \mathbf{v}) = I(\mathbf{B}^+ \mathbf{A}^+ \mathbf{w}; \mathbf{P}_A \mathbf{P}_B \mathbf{v}). \quad (50)$$

Due to the circulant structure of  $\mathbf{P}_A$  and  $\mathbf{P}_B$ , they commute and, therefore,

$$I(\mathbf{P}_B \mathbf{A}^+ \mathbf{w}; \mathbf{P}_A \mathbf{P}_B \mathbf{v}) = I(\mathbf{B}^+ \mathbf{A}^+ \mathbf{w}; \mathbf{P}_B \mathbf{P}_A \mathbf{v}), \quad (51)$$

that is the mutual information in the cost of problem (20). To conclude, we showed the equivalence of the costs (based on the backward-channel construction presented next in Appendix C) and the constraints of problems (18) and (20), therefore, these optimization problems are interchangeable.

#### APPENDIX C

##### THE THEORETIC SETTINGS: EQUIVALENCE OF OPTIMIZATION PROBLEMS (20) AND (21)

Since  $\mathbf{A}$  and  $\mathbf{B}$  are circulant matrices, the expected distortion  $E\{\|\mathbf{AB}(\tilde{\mathbf{w}} - \mathbf{v})\|_2^2\}$ , appearing in the constraint of (20), has the following additively-separable form in the DFT domain

$$\begin{aligned} E\{\|\mathbf{AB}(\tilde{\mathbf{w}} - \mathbf{v})\|_2^2\} &= E\{\|\mathbf{\Lambda}_A \mathbf{\Lambda}_B(\tilde{\mathbf{w}}^F - \mathbf{v}^F)\|_2^2\} \\ &= \sum_{k=0}^{N-1} |a_k^F b_k^F|^2 E\{|\tilde{w}_k^F - v_k^F|^2\}. \end{aligned} \quad (52)$$

This expected distortion formulation motivates us to address the entire rate-distortion optimization in the DFT domain and with respect to a pseudoinverse filtered version of the input  $\mathbf{w}$ . For this purpose we will treat next the optimization cost of the problem given in (20).

Since  $\tilde{\mathbf{w}} \triangleq \mathbf{B}^+ \mathbf{A}^+ \mathbf{w}$  is a cyclo-stationary Gaussian signal, we apply the following familiar lower bounds:

$$I(\tilde{\mathbf{w}}; \mathbf{P}_B \mathbf{P}_A \mathbf{v}) = I(\mathbf{F} \tilde{\mathbf{w}}; \mathbf{F} \mathbf{P}_B \mathbf{P}_A \mathbf{v}) \quad (53)$$

$$= I(\tilde{\mathbf{w}}^F; \mathbf{\Lambda}_{\mathbf{P}_B} \mathbf{\Lambda}_{\mathbf{P}_A} \mathbf{v}^F) \quad (54)$$

$$\geq \sum_{k \in \mathcal{K}_{AB}} I(\tilde{w}_k^F; v_k^F) \quad (55)$$

where (53) is due to the invariance of mutual information under a unitary transformation, (54) exhibits the diagonal forms of the projection matrices, and the bound (55) is due to the independence of the DFT coefficients  $\{\tilde{w}_k^F\}_{k=0}^{N-1}$  stemming from cyclo-stationary Gaussian characteristics of  $\tilde{\mathbf{w}}$ . Moreover, note that (55) refers only to mutual information of DFT components belonging to the range of  $\mathbf{AB}$ , this is due to (54) where  $\mathbf{v}^F$  components corresponding to the nullspace of  $\mathbf{AB}$  are zeroed (hence, they yield zero mutual information and zero rate). The next lower bound emerges from the definition of the rate-distortion function for each of the components, i.e.,

$$\sum_{k \in \mathcal{K}_{AB}} I(\tilde{w}_k^F; v_k^F) \geq \sum_{k \in \mathcal{K}_{AB}} R_k(D_k) \quad (56)$$

$$= \sum_{k \in \mathcal{K}_{AB}} \left[ \frac{1}{2} \log \left( \frac{\lambda_k^{(\tilde{\mathbf{w}})}}{D_k} \right) \right]_+ \quad (57)$$

where the last equality relies on the rate-distortion function formulation for a scalar Gaussian source. The  $k^{th}$  variable here is  $\tilde{w}_k^F$ , having the a variance denoted as  $\lambda_k^{(\tilde{\mathbf{w}})}$ . Here, the  $k^{th}$ -component rate corresponds to an expected squared-error distortion denoted as  $D_k \triangleq E\{|\tilde{w}_k^F - v_k^F|^2\}$ .

The mutual-information lower bound in (57) is further minimized under the total distortion constraint that expresses the weights introduced in (52) for each of the DFT components, i.e., the distortion-allocation optimization is

$$\begin{aligned} \min_{\{D_k\}_{k \in \mathcal{K}_{AB}}} & \sum_{k \in \mathcal{K}_{AB}} \frac{1}{2} \log \left( \frac{\lambda_k^{(\tilde{\mathbf{w}})}}{D_k} \right) \\ \text{s.t.} & \sum_{k \in \mathcal{K}_{AB}} |a_k^F b_k^F|^2 D_k \leq ND \\ & 0 \leq D_k \leq \lambda_k^{(\tilde{\mathbf{w}})}, \quad k \in \mathcal{K}_{AB}. \end{aligned} \quad (58)$$

where the operator  $[\cdot]_+$  in (57) was replaced with componentwise constraints. The optimization (58) is solved using Lagrangian optimization and the KKT conditions. We denote here the optimal distortions as  $\{\hat{D}_k\}_{k=0}^{N-1}$ , where for  $k \notin \mathcal{K}_{AB}$  we set  $\hat{D}_k = 0$ , and use them next for showing the achievability of the mutual-information lower bound.

We define  $\mathbf{\Lambda}_{\hat{D}}$  as the  $N \times N$  diagonal matrix with  $\hat{D}_k$  as the  $k^{th}$  diagonal value. Also recall that  $\mathbf{H} \triangleq \mathbf{AB}$  and the related definitions given above. Consider the following construction for a backward channel producing  $\tilde{\mathbf{w}}$  from  $\mathbf{v}$ . Let

$$\mathbf{v} \sim \mathcal{N}(\mathbf{0}, \mathbf{H}^+ \mathbf{R}_w \mathbf{H}^{+*} - \mathbf{H}^+ \mathbf{F}^* \mathbf{\Lambda}_{\hat{D}} \mathbf{F} \mathbf{H}^{+*}) \quad (59)$$

$$\mathbf{z} \sim \mathcal{N}(\mathbf{0}, \mathbf{H}^+ \mathbf{F}^* \mathbf{\Lambda}_{\hat{D}} \mathbf{F} \mathbf{H}^{+*}) \quad (60)$$

be two independent random vectors, constructing  $\tilde{\mathbf{w}}$  via

$$\tilde{\mathbf{w}} = \mathbf{v} + \mathbf{z}, \quad (61)$$

hence,  $\tilde{\mathbf{w}} \sim \mathcal{N}(\mathbf{0}, \mathbf{H}^+ \mathbf{R}_w \mathbf{H}^{+*})$ , agreeing with  $\tilde{\mathbf{w}} = \mathbf{H}^+ \mathbf{w}$  where  $\mathbf{w} \sim \mathcal{N}(\mathbf{0}, \mathbf{R}_w)$ . Additionally, the construction (59)-(61) leads to

$$\begin{aligned} E\{\|\mathbf{H}(\tilde{\mathbf{w}} - \mathbf{v})\|_2^2\} &= E\{\|\mathbf{H}\mathbf{z}\|_2^2\} \\ &= E\{\mathbf{z}^* \mathbf{H}^* \mathbf{H} \mathbf{z}\} \\ &= E\{\text{Trace}\{\mathbf{z}^* \mathbf{H}^* \mathbf{H} \mathbf{z}\}\} \\ &= E\{\text{Trace}\{\mathbf{H} \mathbf{z} \mathbf{z}^* \mathbf{H}^*\}\} \\ &= \text{Trace}\{\mathbf{H} \mathbf{R}_z \mathbf{H}^*\} \\ &= \text{Trace}\{\mathbf{H} \mathbf{H}^+ \mathbf{F}^* \mathbf{\Lambda}_{\hat{D}} \mathbf{F} \mathbf{H}^{+*} \mathbf{H}^*\} \\ &= \text{Trace}\{\mathbf{F}^* \mathbf{\Lambda}_{\mathbf{H}} \mathbf{\Lambda}_{\mathbf{H}}^+ \mathbf{\Lambda}_{\hat{D}} \mathbf{\Lambda}_{\mathbf{H}}^{+*} \mathbf{\Lambda}_{\mathbf{H}}^* \mathbf{F}\} \\ &= \text{Trace}\{\mathbf{F}^* \mathbf{\Lambda}_{\hat{D}} \mathbf{F}\} \\ &= \text{Trace}\{\mathbf{\Lambda}_{\hat{D}}\} \\ &= ND \end{aligned} \quad (62)$$

that reaches the maximal allowed distortion in (58). We used here the relation  $\mathbf{\Lambda}_{\mathbf{H}} \mathbf{\Lambda}_{\mathbf{H}}^+ \mathbf{\Lambda}_{\hat{D}} \mathbf{\Lambda}_{\mathbf{H}}^{+*} \mathbf{\Lambda}_{\mathbf{H}}^* = \mathbf{\Lambda}_{\hat{D}}$ , emerging from the fact that  $\hat{D}_k = 0$  for components in the nullspace of  $\mathbf{H}$ . This construction fulfills (46), (55) and (56) with equality, thus, proves the equivalence of the optimization problems (18), (20), and (21).



## APPENDIX D

### ADDITIONAL DETAILS ON THE EXPERIMENTS FOR CODING OF ONE-DIMENSIONAL SIGNALS

#### 1) The Tree-based Coding Method for One-Dimensional Signals:

We consider a coding procedure that relies on a nonuniform segmentation of the signal based on a binary tree structure. The method presented here is influenced by the general framework given in [17] for optimizing tree-structures, and by the rate-distortion Lagrangian optimization in [14], [15].

We consider the coding of a  $M$ -length vector  $\mathbf{w} \in \mathbb{R}^M$ , where  $M = 2^{d_0}$  for some positive integer  $d_0$ . The procedure starts with a full  $d$ -depth binary-tree ( $d \leq d_0$ ), which is the initial tree, describing a uniform partitioning of the vector components  $w_k$ ,  $k = 0, \dots, M - 1$ , into  $2^d$  sub-vectors of  $M \cdot 2^{-d}$  length. The segmentation of the vector is represented by the leaves of the binary tree: the sub-vector location and length are determined by the leaf place in the tree, in particular, the sub-vector length is defined by the tree-level that the leaf belongs to. The examined nonuniform segmentations are induced by all the trees obtained by repeatedly pruning neighboring-leaves having the same parent node. The initial  $d$ -depth full-tree together with all its pruned subtrees form the set of relevant trees, denoted here as  $\mathcal{T}_d$ .

The leaves of a tree  $T \in \mathcal{T}_d$  form a set denoted as  $L(T)$ , where the number of leaves is referred to as  $|L(T)|$ . Accordingly, the tree  $T$  represents a (possibly) nonuniform partitioning of the  $M$ -length vector into  $|L(T)|$  segments. A leaf  $l \in L(T)$  resides in the  $h(l)$  level of the tree and corresponds to the indexing interval  $[a_{(l)}^{left}, \dots, a_{(l)}^{right}]$  of length  $\Delta(l) = M \cdot 2^{-h(l)}$ . A segment, corresponding to the leaf  $l \in L(T)$ , is represented by its average value

$$\hat{w}_{(l)} = \frac{1}{\Delta(l)} \sum_{k=a_{(l)}^{left}}^{a_{(l)}^{right}} w_k \quad (63)$$

that is further uniformly quantized using  $q_b = 8$  bits. The quantized sample corresponding to the  $l^{th}$  leaf (segment) is denoted as  $\hat{w}_{(l)}^Q$ . This coding structure leads to reconstruction squared-error induced by the tree  $T \in \mathcal{T}_d$  and calculated based on its leaves,  $L(T)$ , via

$$\mathcal{E}^2(T) = \sum_{l \in L(T)} \sum_{k=a_{(l)}^{left}}^{a_{(l)}^{right}} (w_k - \hat{w}_{(l)}^Q)^2. \quad (64)$$

For a given signal  $\mathbf{w} \in \mathbb{R}^M$  and a budget of  $\rho$  bits, one can formulate the optimization of a tree-structured nonuniform coding as

$$\begin{aligned} & \underset{T \in \mathcal{T}_d}{\text{minimize}} && \mathcal{E}^2(T) \\ & \text{subject to} && q_b |L(T)| = \rho, \end{aligned} \quad (65)$$

namely, the optimization searches for the tree associated with a bit-cost of  $\rho$  bits that provides minimal reconstruction squared-

error. The unconstrained Lagrangian form of (65) is

$$\min_{T \in \mathcal{T}_d} \{ \mathcal{E}^2(T) + \nu (q_b |L(T)|) \}, \quad (66)$$

where  $\nu \geq 0$  is a Lagrange multiplier that corresponds to  $q_b |L(T)| = \rho$ . However, it should be noted that due to the discrete nature of the problem such  $\nu$  does not necessarily exist for any  $\rho$  value (see details, e.g., in [17], [18]). The problem (66) can also be written as

$$\min_{T \in \mathcal{T}_d} \left\{ \sum_{l \in L(T)} \sum_{k=a_{(l)}^{left}}^{a_{(l)}^{right}} (w_k - \hat{w}_{(l)}^Q)^2 + \nu q_b |L(T)| \right\}. \quad (67)$$

Importantly, since the representation intervals do not overlap, the contribution of a leaf,  $l \in L(T)$ , to the Lagrangian cost is

$$C(l) = \sum_{k=a_{(l)}^{left}}^{a_{(l)}^{right}} (w_k - \hat{w}_{(l)}^Q)^2 + \nu q_b. \quad (68)$$

The discrete optimization problem (67) of optimizing the tree for a given signal and a Lagrange multiplier  $\nu$  is practically addressed as follows. Start from the full  $d$ -depth tree and determine the corresponding segments and their quantized samples, squared errors, and contributions to the Lagrangian cost (68). Go through the tree levels from bottom and up, in each tree level find the pairs of neighboring leaves having the same parent node and evaluate the pruning condition: if

$$C(\text{left child}) + C(\text{right child}) > C(\text{parent}) \quad (69)$$

is true, then prune the two leaves – implying that two segments are merged to form a single sub-vector of double length (thus, the total bit-cost is reduced by  $q_b$ ). If the condition (69) is false, then the two leaves (and the associated representation segments) are kept. This evaluation is continued until reaching a level where no pruning is done, or when arriving to the root of the tree.

#### 2) The Experiment Settings used for Adjusting Compression of One-Dimensional Signals to an Acquisition-Rendering System:

The considered source signal  $\mathbf{x}$  is an amplitude-modulated chirp (see the blue curves in Figs. 2a-2b), defined by sampling its mathematical formulation using 1024 samples uniformly spread in the "time" interval  $[0, 1]$ . Note that the chirp signal values are in the range  $[0, 1]$ , a property used in the PSNR computation shown in the result evaluation in Fig. 2c.

The acquisition is modeled here by a low-pass filtering applied using a convolution with a Gaussian kernel (standard deviation 15) and support of 15 samples, followed by sub-sampling in a factor of 4, and an additive white Gaussian noise with standard deviation 0.001. This procedure results with the 256-samples signal  $\mathbf{w}$  that is given to the compression. After decompression the rendering operator is applied by replicating each sample of  $\mathbf{v}$  four times such that the piecewise-constant signal  $\mathbf{y}$  is formed, having a size of 1024 samples.

We tested two compression strategies to employ in the acquisition-rendering system. The first is a regular compression using the tree-based procedure, described in the former subsection, applied based on some Lagrange multiplier  $\nu$ . The experiment for this regular flow was repeated for various values of the Lagrange multiplier  $\nu$  to produce the PSNR-bitrate curve in Fig. 2c. The second approach relied on the implementation of the proposed method (Algorithm 1) as the compression stage that leverages the standard tree-based coding described in the former subsection. This approach was evaluated for a range of  $\nu$  values to obtain the corresponding PSNR-bitrate curve in Fig. 2c. The implementation of our iterative method (Algorithm 1) run a maximum of 40 iterations or until convergence is detected.

## APPENDIX E

### ADDITIONAL DETAILS ON THE EXPERIMENTS FOR VIDEO CODING

The source signal  $\mathbf{x}$  is a sequence of 10 frames, each of  $480 \times 480$  pixels. The acquisition is modeled here by a low-pass filtering carried out by a convolution with a two-dimensional Gaussian kernel (standard deviation 1) and support of  $5 \times 5$  pixels, followed by horizontal and vertical sub-sampling in a factor of 2, and an additive white Gaussian noise with standard deviation 0.001. This procedure results with the 10-frame sequence  $\mathbf{w}$  with a frame size of  $240 \times 240$  pixels. The rendering applied after decompression is simply done by replicating each pixel of  $\mathbf{v}$  in a  $2 \times 2$  pixels square such that the rendered signal  $\mathbf{y}$  has frames of  $480 \times 480$  pixels having spatial piecewise-constant form.

We evaluated two compression approaches to apply in the acquisition-rendering system. One, is to employ a regular compression using the HEVC video coding standard (using its reference software, version HM 15.0, available at <http://hevc.hhi.fraunhofer.de/>). The experiment for this regular approach was repeated for various values of the quality parameter of the HEVC to produce the PSNR-bitrate curve in Fig. 3. The second strategy implemented the proposed method (Algorithm 1) as the compression procedure that utilizes the HEVC standard. This approach was evaluated for a range of HEVC quality parameters to provide the corresponding PSNR-bitrate curve in Fig. 3. The implementation of our iterative method (Algorithm 1) run a maximum of 10 iterations or until convergence is detected.

In Fig. 3 we presented the PSNR-bitrate curves for the compression of segments of two video signals: 'Stockholm' and 'Shields'. Here, in Figures 4 and 5, we show the third frame from the sequence, in its original form and in its rendered form using the regular approach and via the proposed method. Clearly, our method provides a more vivid image (also having higher PSNR) at a lower bit-rate.



Fig. 4. Coding a group of 10 frame from the 'Stockholm' sequence (spatial portion of 480x480 pixels). (a) The third source frame. (b) the rendered frame using regular compression (28.29 dB at 2.37 bpp). (c) the rendered frame using the proposed compression (29.45 dB at 1.34 bpp).

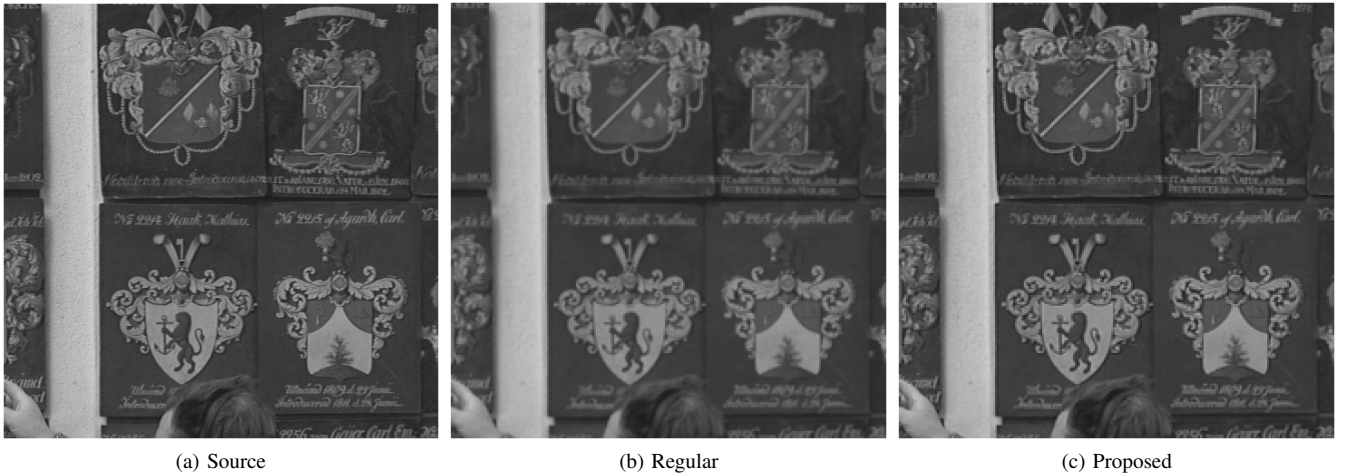


Fig. 5. Coding a group of 10 frame from the 'Shields' sequence (spatial portion of 480x480 pixels). (a) The third source frame. (b) the rendered frame using regular compression (27.93 dB at 2.41 bpp). (c) the rendered frame using the proposed compression (29.31 dB at 1.31 bpp).